An Improved Bidirectional Hybrid Switched Inductor Converter

Dan Hulea[1], Mihaita Gireada[1], Danut Vitan[1], Octavian Cornea[1], Nicolae Muntean[1,2]
[1] Politehnica University of Timisoara [2] Romanian Academy, Timisoara Branch
[1] Piata Victoriei No. 2 [2] Bv. Mihai Viteazu 24
Timisoara, Romania
Tel.: +40-256-403-450
E-Mail: dan.hulea@upt.ro; mihaita.gireada@student.upt.ro; daunt.vitan@upt.ro;
octavian.cornea@upt.ro; nicolae.muntean@upt.ro;
URL: http://www.et.upt.ro/en

Acknowledgements

This work was supported by a grant of the Romanian Ministery of Research and Innovation, CCCDI – UEFISCDI, project number PN-III-P1-1.2-PCCDI-2017- 0391 / CIA_CLIM – "*Smart buildings adaptable to the climate change effects*", within PNCDI III.

This work was also supported by a grant of the Romanian Ministry of Research and Innovation no. 10PFE/16.10.2018, PERFORM-TECH-UPT - The increasing of the institutional performance of the Polytechnic University of Timișoara by strengthening the research, development and technological transfer capacity in the field of "Energy, Environment and Climate Change"

Keywords

«Converter circuit», «Converter control», «DC power supply», « Supercapacitor», « High voltage power converters».

Abstract

This paper proposes an improved high ratio bidirectional hybrid DC-DC converter that incorporates a switched inductor cell which helps achieve wider conversion ratios, reduced components size, and reduced semiconductor stress. The improvements for this topology, when compared to other bidirectional hybrid switched capacitor converters, consist of the elimination of inductor voltage oscillations, reduction of maximum voltage stress on transistors, minimization of parasitic switching inductances and elimination of high frequency common mode voltage. The topology is realized with two conventional half bridges, which help achieve a faster implementation, and provides the topology with the benefit of utilizing the research realized on these structures.

Introduction

High voltage conversion ratio converters are used where a large difference is present between the input and the output voltage levels. High ratio bidirectional converters are useful for storage elements with large voltage variations with respect to their stored energy, such as supercapacitors [1]. Hybrid converters make use of inductive or capacitive switching cells to achieve a wider voltage conversion ratio, lower active switch stress or smaller passive components [2], [3].

Compared to other topologies, the bidirectional hybrid switched inductor converter (BHSI) presented in [4] was proven to have good characteristics, as the ones mentioned above. A significant disadvantage was also found, present in the unidirectional topology as well [3]: large inductor voltage oscillations that translate in switch overvoltage. The scope of this paper is to propose a new, improved, BHSI configuration that overcomes this disadvantage, while introducing additional advantages.

Topology description

The new BHSI converter, presented in Fig. 1, adds an additional switch (S_{L2}) in order to make use of two half bridges, consisting of S_{H1} - S_{L1} and S_{H2} - S_{L2} transistor groups. The use of half bridges and two additional capacitors, C_1 and C_2, introduce multiple benefits, the most notable being (i) the elimination of switch voltage oscillations, (ii) minimization of switching loop parasitic inductances, (iii) simplification of PCB design, and (iv) the use of already available research on these building blocks.

The inductor voltage oscillations appear due to the parasitic capacitance of S_{L1} and S_{H2}, a phenomenon which was previously studied for the unidirectional boost hybrid switched inductor converter in [3]. As presented in the schematic, the improvements for the proposed BHSI are different than [3], because each additional capacitor is connected in parallel to one of the two half bridges, therefore it also minimizes the parasitic inductances within the switching loops (S_{H1} - S_{L1} - C_1 and S_{H2} - S_{L2} – C_2). The use of half bridges has a benefit in the PCB design because of the already available power modules, and the numerous studies based on these structures used as building blocks help for determining specific switching parameters [5]–[7].

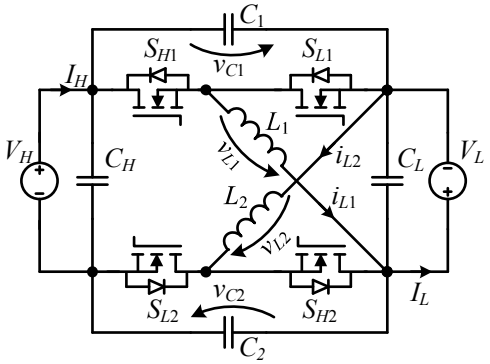

Fig. 1: The proposed BHSI

A few simplifying assumptions are made in order to explain the operation of the BHSI:

- L_1 and L_2 inductors, and their currents (i_{L1} and i_{L2}) are considered identical,
- C_1 and C_2 capacitors, and their voltages (V_{C1} and V_{C2}) are considered identical,
- Capacitors are considered large enough to maintain a constant voltage,
- All components are considered ideal,
- Steady state operation is considered.

Taking into account the simplifying assumptions, the operation of the BHSI can be explained starting from the two equivalent switching states, t_{on} and t_{off}, presented in Fig. 2. During t_{on}, S_{H1} and S_{L2} switches are turned on and S_{H2} and S_{L1} are turned off, so that L_1 and L_2 inductors are connected between the high voltage source, V_H, and the low voltage, V_L. The voltage across C_1 and C_2 is considered:

$$V_{C1} = V_{C2} = \frac{V_H + V_L}{2}, \tag{1}$$

therefore, the voltages across the inductors are:

$$v_{L1} = V_{C1} - V_L = \frac{V_H - V_L}{2}, \tag{2}$$

$$v_{L2} = V_{C2} - V_L = \frac{V_H - V_L}{2}. \tag{3}$$

During t_{off}, the two inductors are connected in parallel to V_L voltage by S_{L1} and S_{H2} transistors, which means that the inductor voltages are:

$$v_{L1} = v_{L2} = -V_L. \tag{4}$$

The main theoretical waveforms, consisting of inductor voltages and currents, input and output currents, and transistor voltages, are presented in Fig. 3. A significant improvement achieved through this topology is the limitation of the maximum voltage on each transistor to a lower value, equal to $(V_H + V_L)/2$.

By applying the inductors volt-second balance:

$$V_{L1} = V_{L2} = D \cdot \frac{V_H - V_L}{2} + (1-D) \cdot (-V) = 0, \tag{5}$$

the relation between the two input voltages is determined:

$$V_L = V_H \cdot \frac{D}{2-D}. \tag{6}$$

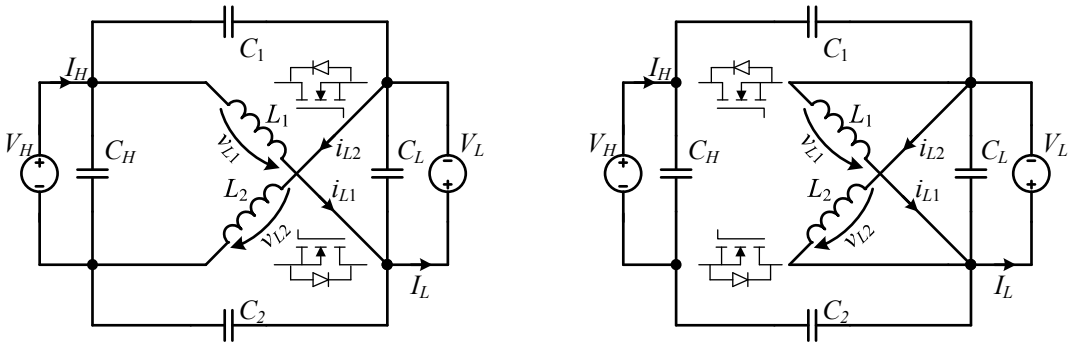

Fig. 2:The two switching states of the BHSI: t_{on} (left) and t_{off} (right)

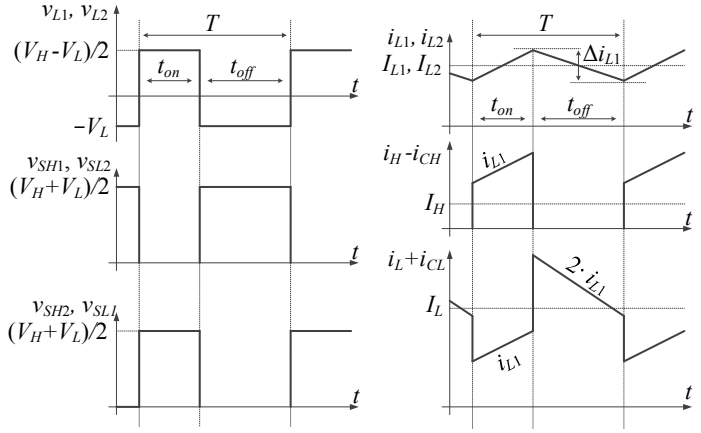

Fig. 3: Main theoretical waveforms of the improved BHSI

Oscillation elimination

Previous papers proposed methods to eliminate the voltage oscillations which appear in the unidirectional topology [3], and experimental results were obtained in the bidirectional topology with oscillations damped by a passive snubber [4]. In this family of topologies, the oscillations are caused by the parasitic capacitors of the transistors in the switching cell, C_{SL1} and C_{SH2} shown in Fig. 4, and the small differences between the switched inductances. The voltage on each transistor will oscillate around the theoretical level with amplitudes and frequencies depending on the values of the resonant circuits. Typical theoretical waveforms are presented in Fig. 5.

The improvement proposed in this paper consists of adding the C_1 and C_2 capacitors and an additional switch, which will eliminate the voltage oscillations by setting a constant voltage between the two voltage sources, V_H and V_L, with a value equal to V_{C1}, from (1). Another benefit is the elimination of the switching frequency voltage between V_H and V_L which was previously present in both unidirectional and bidirectional topologies.

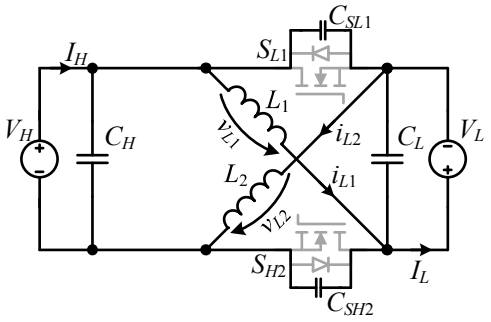

Fig. 4: Equivalent schematic during t_{on} of the unimproved BHSI [4]
(or t_{off} for the unidirectional topology [3])

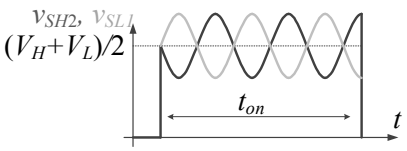

Fig. 5: Transistor voltage waveform during t_{on} state without C_1 and C_2 capacitors
(unimproved BHSI topology)

Comparison of the proposed topology to other converters

In order to compare the proposed BHSI to other topologies, the total inductor energy and the total device stress are used as metrics. To compare the total inductor energy, the inductor currents are calculated using the values of the low voltage side current (I_L) and the duty cycle:

$$I_{L1} = I_L \cdot \frac{1}{2-D} = I_L \cdot \frac{V_L + V_H}{2 \cdot V_H}. \tag{7}$$

The inductor current ripple ratio, r, is used to guarantee that the sizing of the inductors is performed similarly in different topologies. The inductor current ripple is calculated with:

$$\Delta i_{L1} = r \cdot I_{L1}. \tag{8}$$

Considering a constant value for r, the two inductors have the following sizing relation:

$$L_1 = L_2 = \frac{2 \cdot V_H \cdot V_L \cdot (V_H - V_L)}{r \cdot f_{sw} \cdot I_L \cdot (V_H + V_L)^2}. \tag{9}$$

Using (7) and (9), the L_1 inductor energy is expressed as:

$$W_{L1} = \frac{L_1 \cdot {I_{L1}}^2}{2} = \frac{I_L \cdot V_L \cdot (V_H - V_L)}{4 \cdot r \cdot f_{sw} \cdot V_H}, \tag{10}$$

and the total inductor energy can be calculated for any converter with:

$$W_L = \sum_{i=1}^{k} W_{Li} = \sum_{i=1}^{k} \frac{L_i \cdot {I_{Li}}^2}{2}. \tag{11}$$

The total active switch stress is given by:

$$S = \sum_{i=1}^{2} V_{SHi} \cdot I_{SHi} + \sum_{i=1}^{2} V_{SLi} \cdot I_{SLi}, \tag{12}$$

where the maximum voltages (V_{SHi} and V_{SLi}) and currents (I_{SHi} and I_{SLi}) for each transistor are calculated with:

$$V_{SH1} = V_{SL1} = V_{SH2} = V_{SL2} = V_{C1} = V_{C2} = \frac{V_H + V_L}{2}, \tag{13}$$

$$I_{SH1} = I_{SL1} = I_{SH2} = I_{SL2} = I_{L1} = I_{L2} = I_L \cdot \frac{V_L + V_H}{2 \cdot V_H}. \tag{14}$$

The total active switch stress for this topology is:

$$S = I_L \cdot \frac{(V_L + V_H)^2}{V_H}. \tag{15}$$

Even if it has an additional transistor compared to [4], it can be observed that, because of its lower voltage, the total active switch stress is the same. A comparison is presented in Fig. 6 with the relations calculated above, and it is clear that the proposed BHSI has a good conversion ratio, smaller inductors and reduced stress in the active switches.

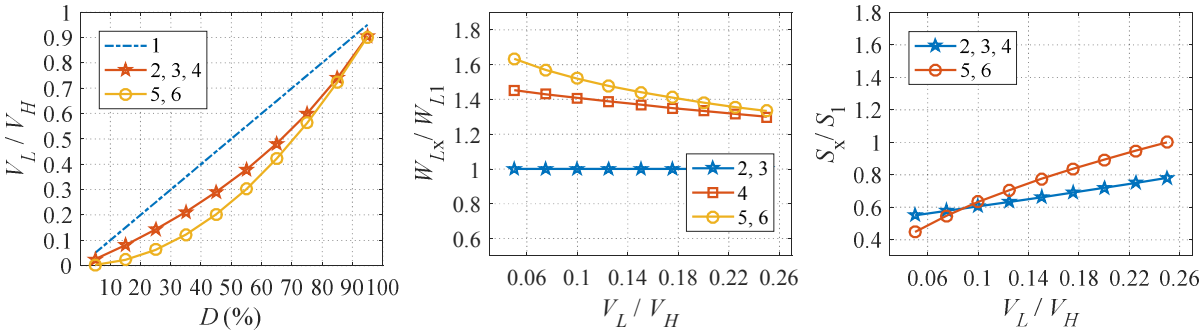

Fig. 6: Comparisons with other topologies (x = 1..6): 1. Conventional Buck/Boost; 2. proposed BHSI; 3. Converter [2]; 4. Converter [1]; 5. Conventional Quadratic [8]; 6. Converter [9]

Simulation and experimental results

The simulations results for the unimproved BHSI topology (without the additional capacitors) present inductor voltage oscillations as discussed in the previous sections, and are presented in Fig. 8. The steady state simulation results for the proposed BHSI from Fig. 8, show that the topology has no inductor voltage oscillations, compared to the conventional structure.

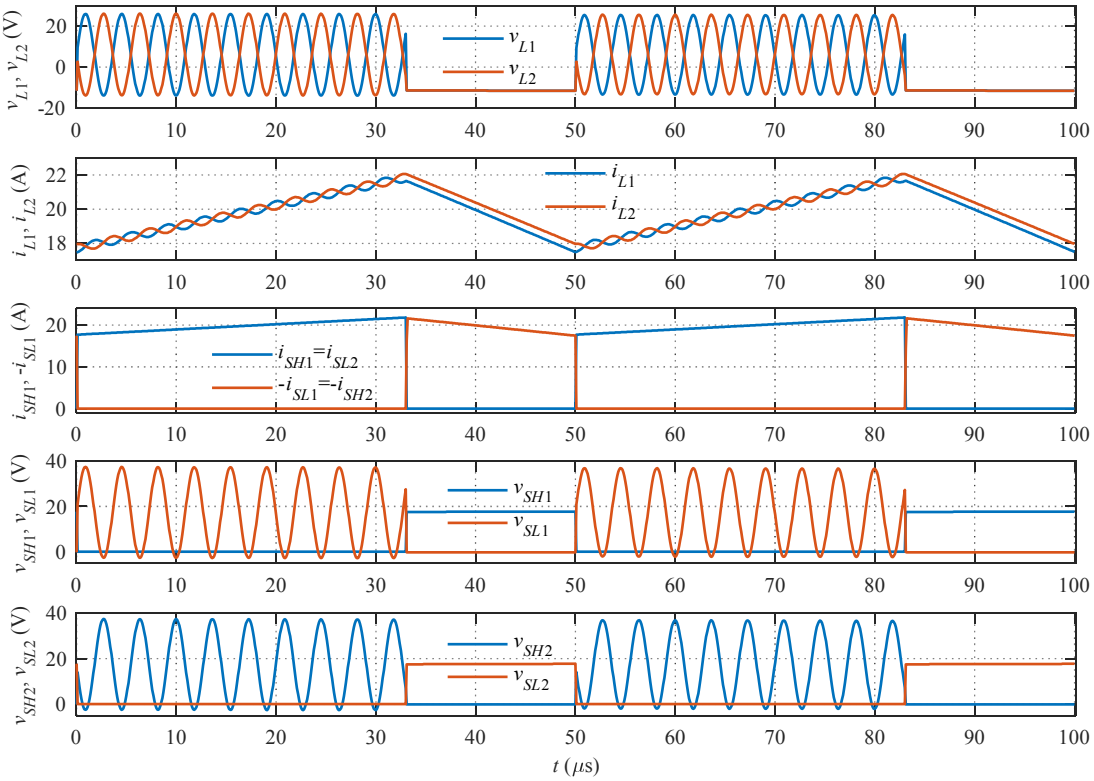

Fig. 7: Steady state simulation results of the unimproved BHSI (without C_1 and C_2)

The simulations for transient operation mode from Fig. 9 present a stable operation with a simple PI controller for i_{L1} current, with a fast transition between buck and boost operation. A small damped oscillation is present in the second inductor current, i_{L2}, which can be ignored, or it can be eliminated with other control strategies.

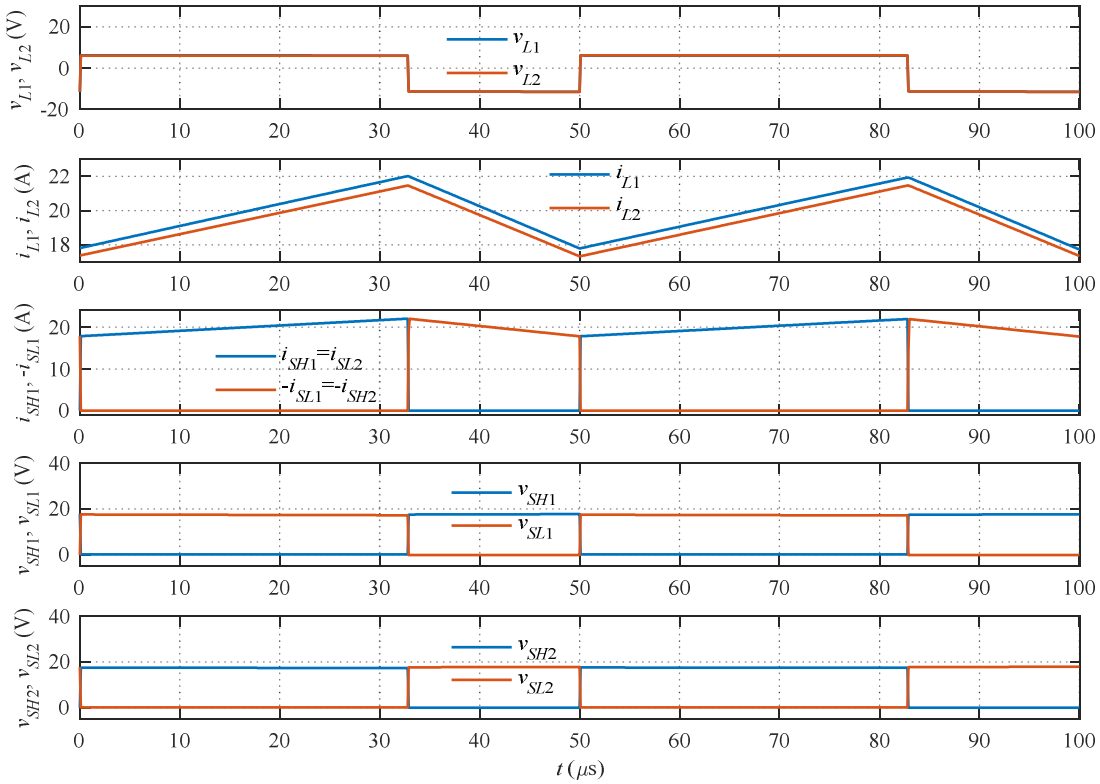

Fig. 8: Steady state simulation results of the proposed BHSI

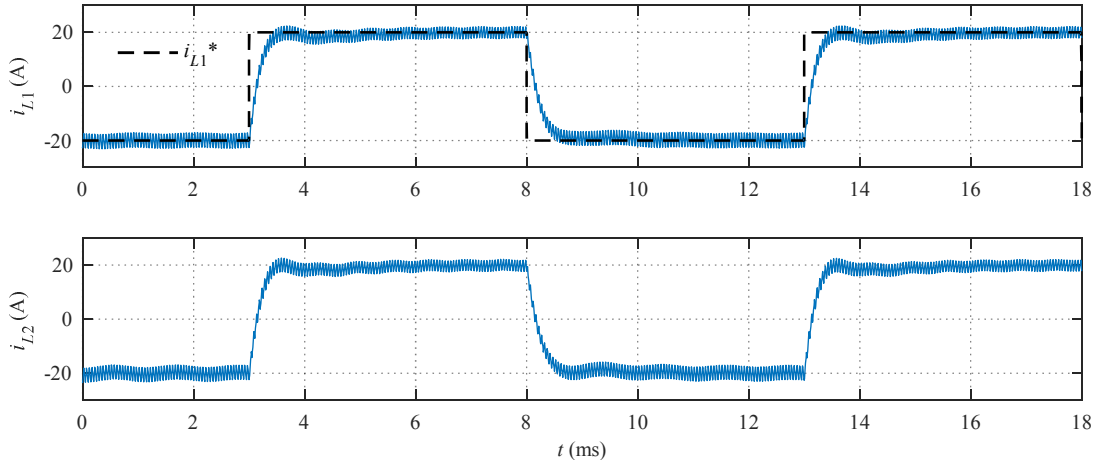

Fig. 9: Transient simulation results i_{L1}* = ± 20 (A)

Steady state experimental results for the proposed BHSI are presented in Fig. 10 to Fig. 12 for both step-up and step-down operation mode. The converter was built and tested with the parameters presented in Table I, having a resistor connected at each respective output (R_{loadH} and R_{loadL}). The inductor voltages and currents presented in Fig. 10, for step-up operation (left) and step-down operation (right) present no oscillations, and are in concordance to the simulation results from Fig. 8.

The voltages on the high side branch switches, v_{SH1} and v_{SL1}, and the voltages on the low side branch switches, v_{SH2} and v_{SL2}, are presented together with the two complementary driving signals, v_{PWM_off}, v_{PWM_on}, in Fig. 11 and Fig. 12, respectively. As the voltage on the inductors do not present any oscillations, the same is valid for the transistor voltages.

Table I: BHSI prototype parameters

Element	V_H	V_L	D	R_{loadH}	R_{loadL}	f	$I_{L1} \approx I_{L2}$	Switches
Value	30	10	50	10	1	20	5.5 / 6.5	BSC040N10NS5
Unit	V	V	%	Ω	Ω	kHz	A	-

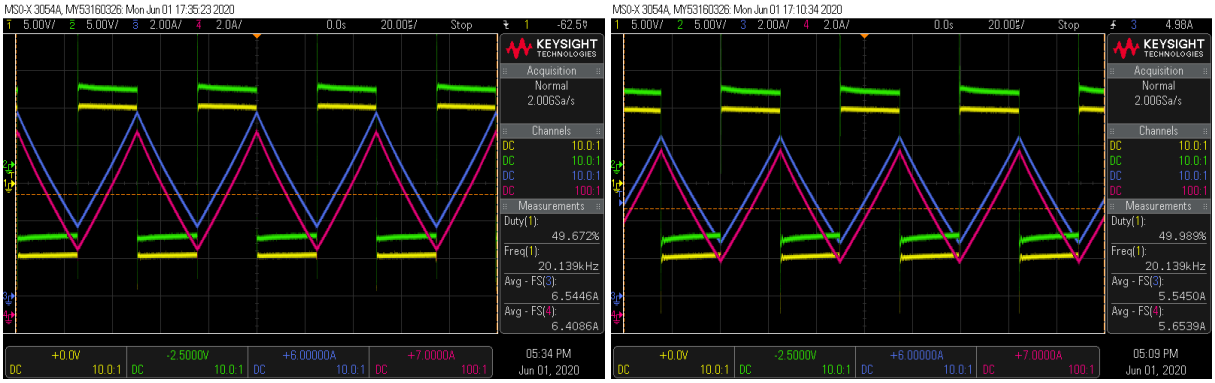

Fig. 10: BHSI experimental results for step-down operation (left) and step-up operation (right), (ch1: v_{L1}, ch2: v_{L2}, ch3: i_{L1}, ch4: i_{L2})

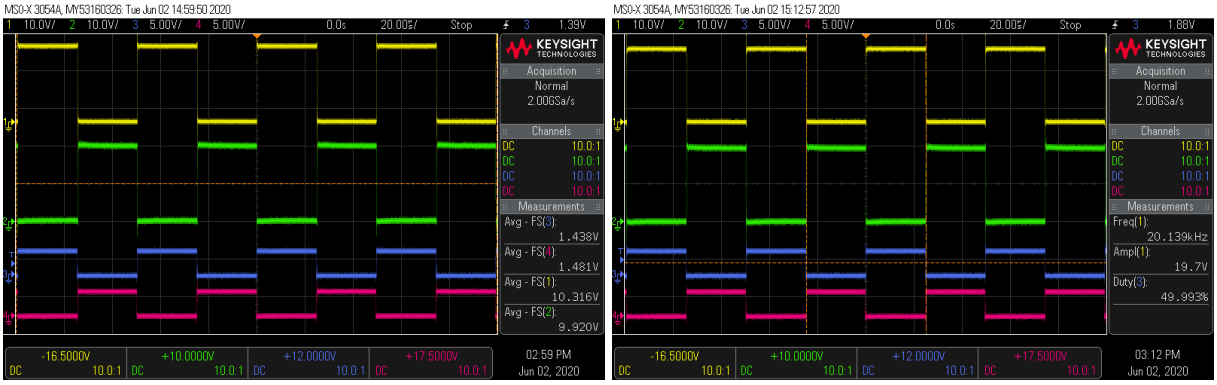

Fig. 11: BHSI experimental results for step-down operation (left), and step-up operation (right) (ch1: v_{SH1}, ch2: v_{SL1}, ch3: v_{PWM_off}, ch4: v_{PWM_on})

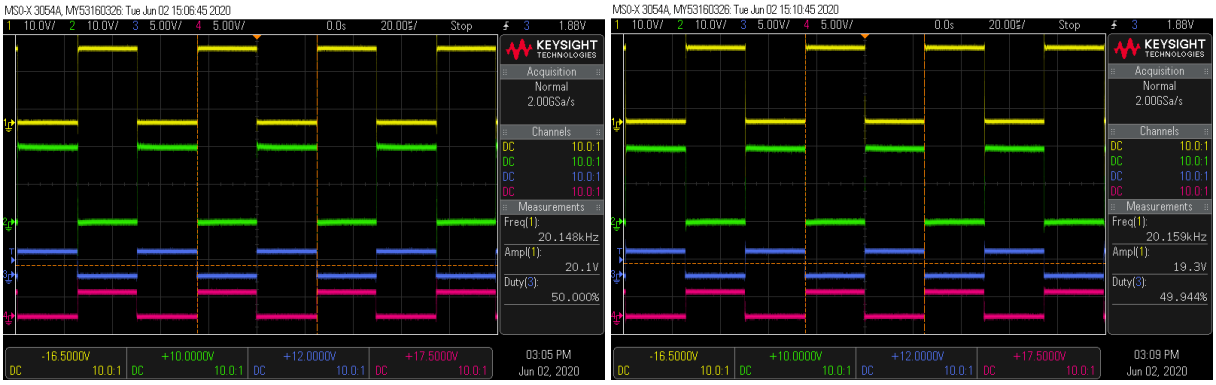

Fig. 12: BHSI experimental results for step-down operation (left), and step-up operation (right) (ch1: v_{SH2}, ch2: v_{SL2}, ch3: v_{PWM_off}, ch4: v_{PWM_on})

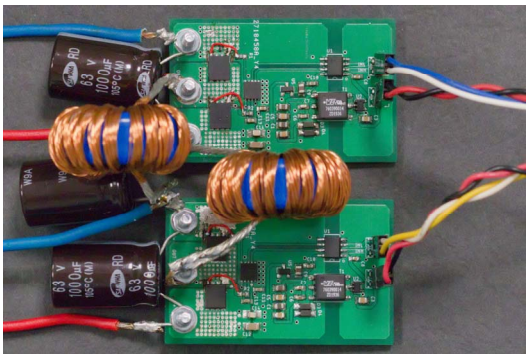

Fig. 13: Prototype of the proposed BHSI converter

Conclusion

This paper presents an improved bidirectional hybrid switched inductor converter which has the advantage of no voltage oscillation in the inductors, a constant DC voltage between the inputs, reduced maximum voltage on the transistors and a reduced inductance in the switching loop. All benefits are introduced by using two half bridges (each in parallel to an additional capacitor) in a way specific to hybrid converters. The topology preserves other benefits introduced by the hybrid switched inductor converters, such as increased voltage conversion ratio, reduced passive component size and reduced stress on the transistors. The characteristics of this topology have been compared to other state of the art structures, and its advantages are highlighted. The simulation results confirm the theoretical assumptions, proving a stable operation in transient regimes, and the experimental results confirm a stable operation without voltage oscillations.

References

[1] Y. Zhang, Q. Liu, J. Li, and M. Sumner, "A Common Ground Switched-Quasi-Z -Source Bidirectional DC–DC Converter With Wide-Voltage-Gain Range for EVs With Hybrid Energy Sources," *IEEE Transactions on Industrial Electronics*, vol. 65, no. 6, pp. 5188–5200, Jun. 2018.

[2] O. Cornea, G. Andreescu, N. Muntean, and D. Hulea, "Bidirectional Power Flow Control in a DC Microgrid Through a Switched-Capacitor Cell Hybrid DC–DC Converter," *IEEE Transactions on Industrial Electronics*, vol. 64, no. 4, pp. 3012–3022, Apr. 2017.

[3] Y. Tang and T. Wang, "Study of An Improved Dual-Switch Converter With Passive Lossless Clamping," *IEEE Transactions on Industrial Electronics*, vol. 62, no. 2, pp. 972–981, Feb. 2015.

[4] D. Hulea, B. Fahimi, N. Muntean, and O. Cornea, "High Ratio Bidirectional Hybrid Switched Inductor Converter Using Wide Bandgap Transistors," in *2018 20th European Conference on Power Electronics and Applications (EPE'18 ECCE Europe)*, 2018, p. P.1-P.10.

[5] J. K. Jorgensen *et al.*, "Loss Prediction of Medium Voltage Power Modules: Trade-offs between Accuracy and Complexity," in *2019 IEEE Energy Conversion Congress and Exposition (ECCE)*, 2019, pp. 4102–4108.

[6] A. B. Jørgensen, T.-H. Cheng, D. Hopkins, S. Beczkowski, C. Uhrenfeldt, and S. Munk-Nielsen, "Thermal Characteristics and Simulation of an Integrated GaN eHEMT Power Module," in *2019 21st European Conference on Power Electronics and Applications (EPE '19 ECCE Europe)*, 2019, p. P.1-P.7.

[7] N. Fichtenbaum, M. Giandalia, S. Sharma, and J. Zhang, "Half-Bridge GaN Power ICs: Performance and Application," *IEEE Power Electronics Magazine*, vol. 4, no. 3, pp. 33–40, Sep. 2017.

[8] A. Ahmad, R. K. Singh, and R. Mahanty, "Bidirectional quadratic converter for wide voltage conversion ratio," in *2016 IEEE International Conference on Power Electronics, Drives and Energy Systems (PEDES)*, 2016, pp. 1–5.

[9] H. Ardi, A. Ajami, F. Kardan, and S. N. Avilagh, "Analysis and Implementation of a Nonisolated Bidirectional DC–DC Converter With High Voltage Gain," *IEEE Transactions on Industrial Electronics*, vol. 63, no. 8, pp. 4878–4888, Aug. 2016.